Atomic structure and optical anisotropy of III–V(001) surfaces

N. Esser[a)]
Institut für Festkörperphysik, Technische Universität Berlin, Hardenbergstraße 36, 10623 Berlin, Germany

W. G. Schmidt
IFTO, Friedrich-Schiller-Universtität Jena, Max-Wien-Platz 1, 07743 Jena, Germany

C. Cobet and K. Fleischer
Institut für Festkörperphysik, Technische Universität Berlin, Hardenbergstraße 36, 10623 Berlin, Germany

A. I. Shkrebtii
Department of Physics, University of Toronto, Toronto, Ontario, Canada M5S 1A7

B. O. Fimland
Department of Physical Electronics, Norwegian University of Science and Technology, NTNU 7034, Trondheim, Norway

W. Richter
Institut für Festkörperphysik, Technische Universität Berlin, Hardenbergstraße 36, 10623 Berlin, Germany

(Received 26 March 2001; accepted 25 June 2001)

The optical anisotropy of materials with isotropic bulk crystal structure depends to a large extent on the surface atomic structure. For instance, data obtained by reflectance anisotropy spectroscopy (RAS) on (001) surfaces of zinc blende semiconductors such as InP and GaAs, have a fingerprint character for the various surface reconstructions. Here we present RAS spectra for GaAs(001) and InP(001) recorded at room temperature and at low temperature. We show that by comparison with a theoretical analysis based on *ab initio* density functional theory in local-density approximation calculations the origin of characteristic spectral features can be identified and thus RAS spectra utilized to discriminate between different competing structural models. We identify contributions related to electronic transitions between surface states as well as features arising from surface perturbed bulk wave functions. We explain the high sensitivity of RAS to the surface structure and chemistry as due to the surface state related features. © *2001 American Vacuum Society.* [DOI: 10.1116/1.1394730]

I. INTRODUCTION

The experimental characterization of surfaces is still mostly performed with ''classical'' surface science techniques such as electron spectroscopy and scanning tunneling microscopy. In recent years, however, optical spectroscopy techniques are more and more advancing into this field. On the one hand, the improvement of numerical methods in surface theory, which allows us to understand the surface optical response in terms of microscopic surface excitations (electronic transitions within the surface band structure), has stimulated applications of optical spectroscopy, for surface characterization. On the other hand, optical spectroscopy, different than the well established electron based surface science techniques, can also be applied to surfaces in non-ultrahigh vacuum (UHV) environments.

Rather widely used is reflectance anisotropy spectroscopy (RAS), also termed reflectance difference spectroscopy. RAS is a powerful tool for characterizing static surfaces as well as for monitoring dynamic surface processes in various environments.[1,2] Because of its broad applicability, much work has been dedicated to clarify the origin of the reflectance anisotropy. More than a decade ago it was shown that the optical anisotropy is partly related to electronic surface states.[3] Aspnes and Studna[4] discriminated between two RAS components: ''intrinsic'' contributions from surface effects on bulk wave functions and ''extrinsic'' contributions related to the surface electronic structure. The latter are particularly interesting from surface science as well as a technological point of view, as they give rise to the correlation between atomic surface structure and optical anisotropy. Meanwhile, the understanding of surface optical properties has improved by calculating the spectral response on the base of surface electronic band structures derived for realistic atomic surface structures. A combination of *first-principles* total-energy (TE) calculations for atomic structure with tight-binding calculations for electronic structure was applied to GaAs(001).[5] Recently, a more accurate theoretical modeling was achieved for InP(001) using a full *ab initio* modeling.[6]

In this article we discuss experimental and theoretical work obtained on GaAs(001) and InP(001) to outline the microscopic understanding of surface optical properties which may be achieved. We show that the surface optical anisotropy may be utilized for discriminating between competing surface structure models.

II. EXPERIMENTAL AND COMPUTATIONAL METHODS

The InP(001) and GaAs(001) surfaces were prepared in UHV by thermal desorption of protective arsenic or phos-

[a)]Author to whom correspondence should be addressed; electronic mail: Norbert.Esser@physik.tu-berlin.de

phorous cap layers.[7–9] The samples (capped homoepitaxial epilayers) were grown by molecular beam epitaxy or metal-organic vapor phase epitaxy. After preparation the surfaces were investigated at room temperature (RT) by low energy electron diffraction, Auger electron spectroscopy, scanning tunneling microscopy, and reflectance anisotropy spectroscopy (RAS). RAS experiments were carried out at room temperature as well as at low temperature (LT) (approximately 30–40 K).

The total-energy (TE) calculations were based on density-functional theory in local-density approximation (DFT-LDA). Using the atomic positions of the relaxed ground state obtained from this total-energy minimization, the optical spectra were calculated in an independent-particle approximation. We apply either an empirical tight binding approximation or use directly the DFT-LDA electronic structure. In the latter case self-energy effects are included via the so-called GW approach (GWA).[31,32] In GWA the self-energy operator Σ is approximated by the convolution of the single-particle propagator G (Green's function) and the screened Coulomb potential W. To calculate W we use a model dielectric function. Thus our GW model requires the input of the dielectric constant ϵ_∞. However, it has been shown that the inaccuracies caused by the use of a bulk dielectric constant for surface GW calculations are very small.[10] To determine the optical anisotropy we follow the formalism developed by Del Sole[11] and Manghi *et al.*[12] Computational details can be found in Refs. 13, 14, and 30.

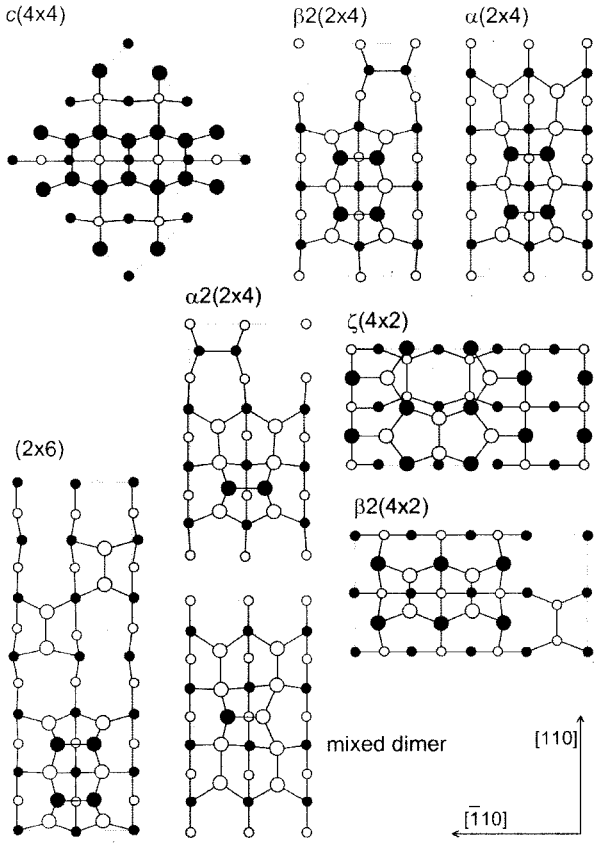

FIG. 1. Top view of relaxed (001) surface structures. Empty and filled circles represent group III and group V atoms, respectively. Positions in the uppermost two atomic layers are indicated by larger symbols.

III. RESULTS AND DISCUSSION

A. GaAs(001)

During recent years, much experimental work has concentrated on GaAs(001) surfaces. GaAs has been considered as a prototype material to clarify the structures of the technologically important (001) surfaces of III–V semiconductors. A variety of different reconstructions, depending on surface stoichiometry, are known on GaAs(001).[15] In particular the three so-called "main" reconstructions, i.e., the As-rich $c(4\times4)$, the As-rich $(2\times4)/c(2\times8)$, and the Ga-rich $(4\times2)/c(8\times2)$ (shown in Fig. 1) were characterized very intensively.[15–17]

Nevertheless, recently it has been demonstrated that the assumption of similar surface structures for the (001) surfaces of different III–V materials is not correct. On (001) surfaces of InP and GaP (2×1) reconstructions for P termination and (2×4) reconstructions for III. (Ga or In) termination have been found. Among these only the atomic structures of the Ga or In-terminated (2×4) reconstructions have been clarified so far. Its key element, the so-called "mixed dimer," consisting of one group III and one group V element, is unknown on III-As(001) surfaces (see mixed dimer structure in Fig. 1). Moreover, on AlSb(001) and GaSb(001) surfaces new structures have been found. Some of them do not fulfill the electron counting rule[18] and others contain mixed dimers.[19] These discrepancies seem to be correlated to surface strain induced by the restructuring at the surface.[20] In realistic structures derived from total energy calculations, some of the atoms in the second, third, or forth atomic layers are considerably displaced from the atomic position in the bulk crystal structure, due to strain. Since atomic radii of the elemental constituents vary for different III–V materials, different types of surface structures become thus evident.[20]

In a very recent work by Lee, Moritz, and Scheffler a new type of surface structure has been proposed for Ga-rich GaAs(001).[21] This structure, called ζ-(4×2) structure, is shown in Fig. 1 together with a variety of structure models discussed in previous literature. All these structures have been optimized and tested for their stability by *ab initio* total energy (TE) calculations.[22] The resulting surface phase diagram is shown in Fig. 2. The TE calculations confirm the well-known structures occurring on As-rich surfaces: The most As-rich structure is the $c(4\times4)$ surface, for less As-rich conditions the $\beta2(2\times4)$ structure is favored. The $\beta2(4\times2)$ structure, to the contrary, is far above the energy of stable surface structures and thus not realistic. As first shown by Lee and co-workers[21], the $\zeta-(4\times2)$-structure has a considerably lower total energy under Ga-rich condition. Only under extreme Ga-rich conditions the mixed dimer (2×4) structure appears to be lower in the TE calculations.

In spite of the TE result, the latter mixed dimer (2×4) structure does not exist on the real GaAs(001) surface since experimental studies do not reveal a (2×4) surface symmetry

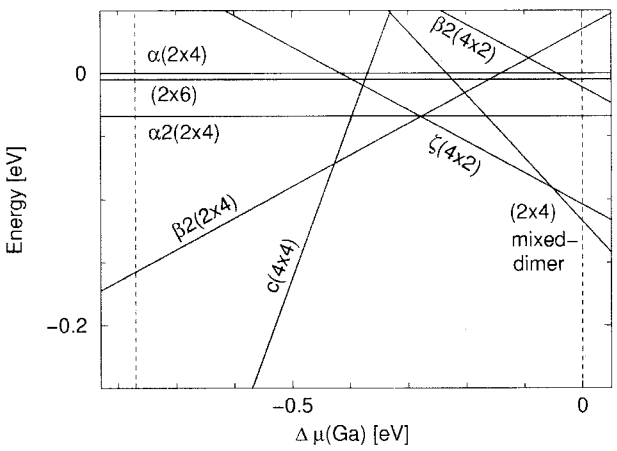

FIG. 2. Relative formation energy per (1×1) unit cell for the different GaAs(001) structure models. Dashed lines mark the approximate anion- and cation-rich limits of the thermodynamically stable range.

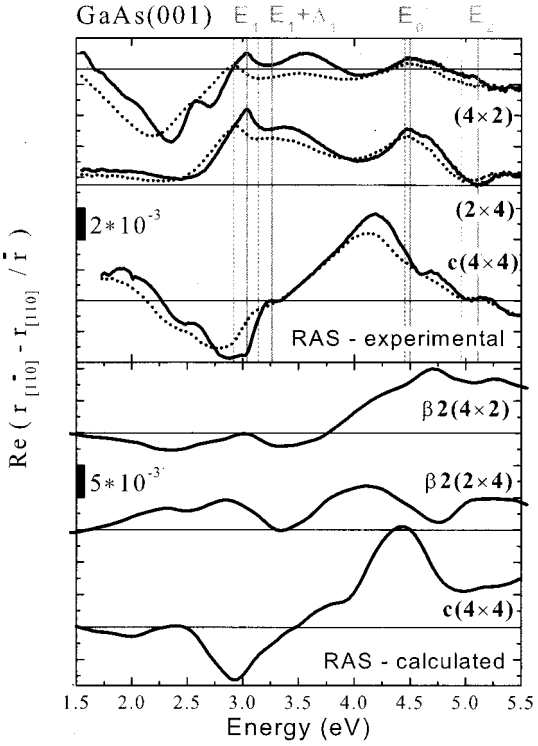

FIG. 3. Experimental and calculated RAS spectra for the three main GaAs(001) reconstructions. The experimental data were recorded *in situ* after decapping and subsequent annealing of undoped GaAs(100). The spectra were taken at room temperature (dashed lines) and at 40 K (full lines). The thin horizontal lines denote the zero levels for each spectrum.

under Ga-rich conditions. This result underlines that the total energy calculations must be taken with care, since they allow a comparison only among a number of suggested structure models which must not necessarily contain the true minimum energy structure for a certain surface stoichiometry. Therefore, a comparison between experimental and theoretical results is very essential to identify the true surface structures.

For this purpose we compare the surface optical anisotropy determined by RAS with calculated spectra obtained for the various atomic structures from TE calculations. In Fig. 3 RAS spectra obtained at room temperature and at 40 K for the $c(4\times4)$, (2×4), and (4×2) surface structures are shown in the upper part. In the lower part calculated spectra are shown which are obtained for the three main reconstructions, i.e., $c(4\times4)$, $\beta2(2\times4)$, and $\beta2(4\times2)$. The RAS spectra were calculated by the empirical tight binding method, based on the atomic structures from *ab initio* total-energy calculations. The experimental spectra demonstrate that the optical anisotropy is indeed characteristic for the surface structure. Supposing the underlying structure model is correct, the calculated spectra should resemble the experimental ones. A strong similarity in line shape is in fact observed between experiment and calculation for the As-rich $c(4\times4)$ structure and to a lesser degree for the (2×4) structure. For the Ga-rich (4×2) structure the experimental spectrum is not reproduced at all. These results infer that the atomic structure of the As-rich reconstructions correspond to the real surface structures whereas the Ga-rich surface is not supported.

In the low-temperature (LT) data in Fig. 3 spectral features are blueshifted and significantly sharpened. The cooling leads to the appearance of new, pronounced structures related to surface transitions, in particular for the $c(4\times4)$ and (4×2) structures. On the (2×4) structure, in contrast, only a sharpening and increase of the spectral features is observed. On this surface the pronounced features are correlated to the E_1, $E_1+\Delta_1$, E_0', and E_2 critical points (CP) of the bulk electronic structure at 3.04, 3.26, 4.5, and 5.1 eV, respectively.

B. InP(001)

The atomic and electronic structure[23–25] of the In-rich InP(001) surface was only recently clarified. In contrast to previous expectations it was found that the group-III-rich surface is not of (4×2) symmetry as in the case of GaAs(001) but shows a (2×4) periodicity.[24] The surface reconstructs in the so-called mixed-dimer-(2×4) structure. Mixed In–P dimers, oriented along $[\bar{1}10]$, terminate the surface (see "mixed dimer" structure in Fig. 1), and In–In bonds along [110] are located in the second layer.

Results for the optical anisotropy measured at RT and LT are shown in the upper part of Fig. 4. The room temperature data agree with earlier findings:[26–28] There is a strong negative anisotropy around 1.8 eV and further features appear close to the E_1 and E_0' critical point (CP) energies. As expected, the low temperature spectrum is blueshifted with respect to the 300 K measurement and a sharpening of the peaks occurs. In addition, features that are hardly discernible at 300 K become prominent, similar as discussed above for GaAs(001). The negative anisotropy at low energies splits into peaks at 1.9, 2.1, and 2.6 eV (denoted S_1, S_2, and S_3) and a positive shoulder (denoted as S_2') develops at 2.3 eV.

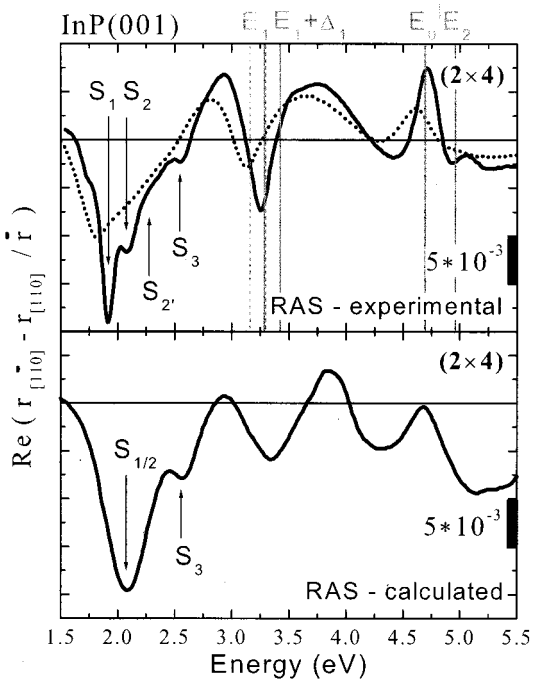

FIG. 4. RAS spectra for the In-rich InP(001)(2×4) surface. The calculated spectra are obtained within a GW approximation. Measurements were performed at 300 (dashed line) and 30 K (full lines). Bulk CP energies and surface-related features are indicated.

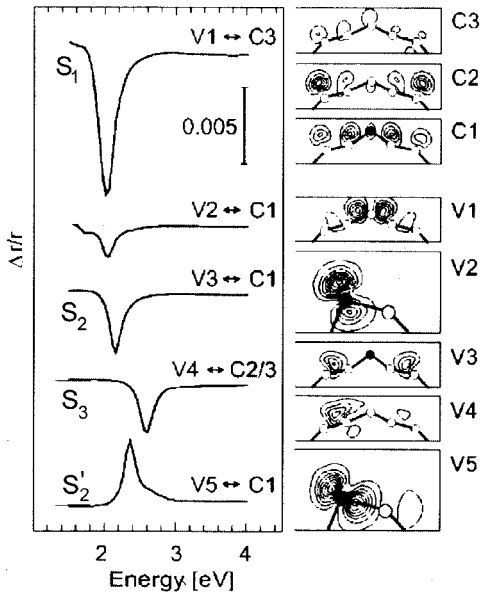

FIG. 5. Left: calculated RAS due to transitions between specific surface states as indicated. Right: orbital character of the corresponding states at K (spacing 10^{-3} Bohr^{-3}).

In the lower part of Fig. 4 a calculated RAS spectrum is shown using the LDA-DFT calculations with GW approximation. The GW corrections are important to yield realistic optical spectra if the DFT-LDA approach is used.[6] Applying the GW correction to InP opens the E_0 gap at $\bar{\Gamma}$ from 0.9 to 1.4 eV. The transition energies E_1 and E_0' are shifted from 2.5 to 3.2 eV and from 4.2 to 5.0 eV, respectively.[6] These values are in good agreement with the E_0, E_1, and E_0' energies of 1.4, 3.3, and 4.8 eV measured by spectroscopic ellipsometry at 30 K.[33] For low photon energies we obtain two pronounced negative peaks (denoted $S_{1/2}$ and S_3). In the high energy region features appear close to the E_1 and E_0' CP energies. Together they form a characteristic ''three-buckle'' shape. We would like to note that the spin-orbit interaction is not taken into account in our calculation. This explains the small differences in line shape between experiment and calculation occurring at the E_1 and E_0' bulk critical points. Apart from this an excellent agreement between GW calculations and experimental spectra is obtained.

Separating spatially the contributions to the optical anisotropy from different slab regions, we find that S_1, S_2, S_2', and S_3 originate entirely from the uppermost four atomic layers. This is consistent with the experiment. The measured negative anisotropy for low energies is extremely dependent on surface structure and therefore surface related, as revealed by RAS data obtained on differently prepared InP(001) surfaces.[26–29] The features at the CP energies arise from transitions between bulk-like electronic states that are perturbed by the surface. In earlier calculations[13] we have shown that these features at the bulk CP energies are rather insensitive to the atomic surface structure. In agreement, RAS experiments performed on differently terminated InP(001) surfaces show very little effect on the three-buckle line shape.[26–28]

An intuitive understanding of surface state ''signatures'' is gained by calculating the optical anisotropy due to transitions within pairs of the above identified surface states. We find that some of these transitions give rise to pronounced anisotropy features. Their superposition nearly accounts for the entire surface contribution to the spectrum. Figure 5 shows the calculated contribution to the RAS from transitions involving $V1-5$ and $C1-3$. This analysis provides a full understanding of the surface features of the optical anisotropy of the In-rich InP(001) surface: S_1 is caused by the bonds between first- and second-layer cations. S_2 arises from transitions mainly involving the second-layer In–In bonds. The symmetry break induced by the mixed dimer on the In–In bonds of the second atomic layer is responsible for S_3, and the dimer bond itself for S_2'. The numerical analysis is consistent with an heuristical interpretation of RAS based on the symmetry of initial and final states: Assuming a larger polarizability along the bond direction, negative anisotropies are expected for the In–In bonds, oriented along $[1\bar{1}0]$, and positive features for the dimer bond, oriented along $[110]$.

C. Dielectric anisotropy

Since the RAS spectra depend both on the optical properties of the surface layer and the underlying bulk of a material, a more direct measure of the surface electronic structure can be obtained by analyzing the data in terms of a three-layer model consisting of the isotropic bulk, the anisotropic surface layer, and the vacuum surrounding. Assuming that the thickness d of the anisotropic surface layer is only a few

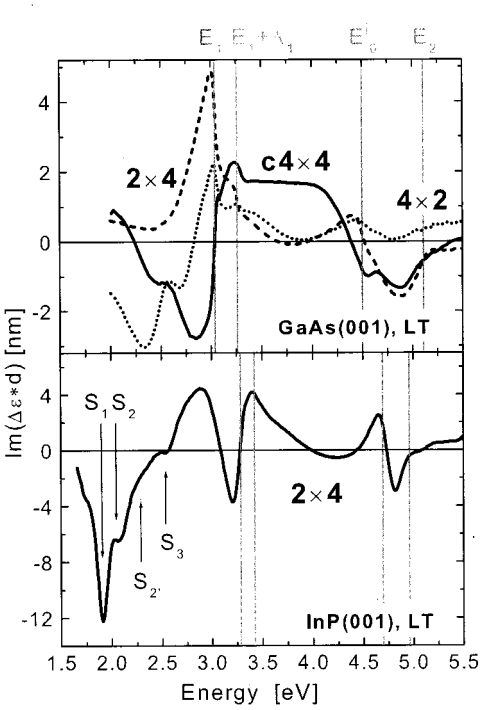

FIG. 6. Surface dielectric anisotropy obtained at 40 K for the three main GaAs(001) reconstructions (upper panel) and for the mixed-dimer InP(001)(2×4) reconstruction (lower panel). The positions of the bulk interband critical points at 40 K is marked by vertical lines. Structures due to surface transitions occur in the spectral region below the E_1 gaps of either materials.

atomic layers, the corresponding surface dielectric anisotropy $\Delta\epsilon$ can rather simply be calculated using the approximation[34]

$$\Delta\epsilon \cdot d = \frac{\lambda}{4\pi i}(\epsilon_b - 1)\frac{\Delta r}{r}. \quad (1)$$

Here ϵ_b denotes the bulk dielectric function. For comparing experimental RAS data with calculations it does not matter whether the dielectric anisotropy or the raw spectra are taken since both quantities can be delivered by the calculations. The interpretation of experimental data such as the ''transition energies'' of surface state related transitions (corresponding to critical points in the surface band structure), however, is more accurate using the surface dielectric anisotropy approximation.

The dielectric anisotropy obtained at LT for the three GaAs reconstructions and the InP(2×4) reconstruction is shown in Fig. 6. The dielectric functions ϵ_b of GaAs and InP bulk materials were taken from Lautenschlager *et al.*[35,36] Apart from the bulk related structures at the E_1, $E_1+\Delta_1$, E_0' and E_2-critical points which are common on all surface structures, individual features related to the surface are evident in the spectral region below the respective E_1 gaps. On GaAs(001) surface structures appear at 2.35 and 2.69 eV for the (4×2), at 2.35, 2.69, and a broad structure around 3.5–4.3 eV for the $c(4\times4)$ reconstruction. The (2×4) surface reconstruction, to the contrary, does not show pronounced surface related features. On InP(001) surface structures arise at 1.91, 2.06, 2.3, and 2.54 eV. The line shape of the optical anisotropy of the Ga-terminated GaAs(4×2) surface is partly similar to that of the In-terminated InP(001)(2×4) surface, despite the rather different surface structure. However, microscopic structural elements such as a covalent bond along the [110] direction between a group V and a group III atom and a covalent bond between two group III atoms along the [110] direction are characteristic of both the mixed-dimer-(2×4) structure and the ζ-(4×2) structure. Therefore the minimum/maximum/minimum structure denoted as $S_2/S_2'/S_3$ on InP(001) involving the surface states V5, V4, and V3 may occur for the GaAs ζ-(4×2) structure as well. The large minimum S1 on InP(001), to the contrary, should not occur on the GaAs ζ-(4×2) structure since there is no structural counterpart for the bonding surface state $V1$ derived from In–In back bonds. This heuristic interpretation in fact explains well the experimental spectrum. In order to achieve a decisive assignment, GW calculations as discussed above for InP(001) of course would be very helpful.

IV. CONCLUSIONS

Combining experimental RAS spectra and results of numerical calculations, we have gained insight into structure determination by optical spectroscopy and shown how the spectral features can be related to electronic transitions within the surface and bulk electronic band structure. Using the differently reconstructed GaAs(001) surfaces as an example, we show that the RAS response is dependent on the real atomic structure and thus a sensitive test of structure models. Extrinsic and intrinsic contributions due to electronic transitions involving surface and bulk electronic states are separated. Low temperature spectra are particularly useful to identify spectral features related to surface electronic transitions. The mixed dimer structure of InP(001)(2×4) serves as a model case to achieve a quantitative agreement between calculation and experiment. For this structure the extrinsic anisotropy features were traced back to transitions involving specific occupied and unoccupied surface states of the uppermost two atomic layers.

ACKNOWLEDGMENTS

The authors acknowledge support by the DFG within the project Es 127/4-1, the BMBF within the Verbundprojekt 22, and grants of computer time from the Leibniz-Rechenzentrum München, the John von Neumann-Institut Jülich, and the Höchstleistungsrechenzentrum Stuttgart.

Presented at the 28th PCSI Conference, Lake Buena Vista, FL, 7–11 January 2001.

[1] I. Kamiya, D. E. Aspnes, L. T. Florez, and J. P. Harbison, Phys. Rev. B **46**, 15894 (1992).
[2] W. Richter and J. T. Zettler, Appl. Surf. Sci. **101**, 465 (1996).
[3] P. Chiaradia, A. Cricenti, S. Selci, and G. Chiarotti, Phys. Rev. Lett. **52**, 1145 (1984).
[4] D. E. Aspnes and A. A. Studna, Phys. Rev. Lett. **54**, 1956 (1985).
[5] A. Shkrebtii, N. Esser, W. Richter, W. G. Schmidt, F. Bechstedt, B. O. Fimland, A. Kley, and R. Del Sole, Phys. Rev. Lett. **81**, 721 (1998).

[6]W. G. Schmidt, N. Esser, A. M. Frisch, P. Vogt, J. Bernholc, F. Bechstedt, M. Zorn, Th. Hamnappel, S. Visbeck, F. Willig, and W. Richter, Phys. Rev. B **61**, R16335 (2000).
[7]U. Resch-Esser, N. Esser, D. Wang, M. Kuball, J. Zegenhagen, M. Cardona, and B. O. Fimland, Surf. Sci. **352–354**, 71 (1996).
[8]N. Esser, U. Resch-Esser, M. Pristovsek, and W. Richter, Phys. Rev. B **53**, R13257 (1996).
[9]K. Knorr, M. Pristovsek, U. Resch-Esser, N. Esser, M. Zorn, and W. Richter, J. Cryst. Growth **170**, 230 (1997).
[10]J. E. Northrup, Phys. Rev. B **47**, 10032 (1993).
[11]R. Del Sole, Solid State Commun. **37**, 537 (1981).
[12]F. Manghi, R. Del Sole, A. Selloni, and E. Molinari, Phys. Rev. B **41**, 9935 (1990).
[13]W. G. Schmidt, E. Briggs, J. Bernholc, and F. Bechstedt, Phys. Rev. B **59**, 2234 (1999).
[14]W. G. Schmidt, Appl. Phys. A: Mater. Sci. Process. **65**, 581 (1997).
[15]L. Däweritz and R. Hey, Surf. Sci. **236**, 15 (1990); D. K. Biegelsen *et al.*, Phys. Rev. B **41**, 5701 (1990).
[16]J. E. Northrup and S. Froyen, Phys. Rev. B **50**, 2015 (1994).
[17]W. G. Schmidt and F. Bechstedt, Surf. Sci. Lett. **76**, L473 (1996).
[18]L. J. Whitman, P. M. Thibado, S. C. Erwin, B. R. Bennett, and B. V. Shanabrook, Phys. Rev. Lett. **79**, 693 (1997).
[19]W. Barvosa-Carter, A. S. Bracker, J. C. Culbertson, B. Z. Nosho, B. V. Shanabrook, L. J. Whitman, H. Kim, N. A. Modine, and E. Kaxiras, Phys. Rev. Lett. **84**, 4649 (2000).
[20]S. Mirbt, N. Moll, K. Cho, and J. D. Joannopolous, Phys. Rev. B **60**, 13283 (1999).
[21]S. H. Lee, W. Moritz, and M. Scheffler, Phys. Rev. Lett. **85**, 3890 (2000).
[22]W. G. Schmidt, S. Mirbt, and F. Bechstedt, Proceedings of 25th International Conference on the Physics of Semiconductors, Osaka, Japan, 2000.
[23]C. D. MacPherson, R. A. Wolkow, C. E. J. Mitchell, and A. B. McLean, Phys. Rev. Lett. **77**, 691 (1996).
[24]W. G. Schmidt, F. Bechstedt, N. Esser, M. Pristovsek, Ch. Schultz, and W. Richter, Phys. Rev. B **57**, 14596 (1998).
[25]P. Vogt, A. M. Frisch, Th. Hannappel, S. Visbeck, F. Willig, Ch. Jung, N. Esser, W. Braun, and W. Richter, Phys. Status Solidi B **215**, 737 (1999).
[26]D. Pahlke, J. Kinsky, Ch. Schultz, M. Pristovsek, M. Zorn, N. Esser, and W. Richter, Phys. Rev. B **56**, R1661 (1997).
[27]M. Zorn, T. Trepk, J.-T. Zettler, B. Junno, C. Meyne, K. Knorr, T. Wethkamp, M. Klein, M. Miller, W. Richter, and L. Samuelson, Appl. Phys. A: Mater. Sci. Process. **65**, 333 (1997).
[28]K. B. Ozanyan, P. J. Parbrook, M. Hopkinson, C. R. Whitehouse, Z. Sobiesierski, and D. I. Westwood, J. Appl. Phys. **82**, 474 (1997).
[29]T. Hannappel, S. Visbeck, M. Zorn, J. T. Zettler, and F. Willig, J. Cryst. Growth **221**, 124 (2000).
[30]E. L. Briggs, D. J. Sullivan, and J. Bernholc, Phys. Rev. B **54**, 14362 (1996).
[31]M. S. Hybertsen and S. G. Louie, Phys. Rev. B **34**, 5390 (1986).
[32]F. Bechstedt, R. Del Sole, G. Cappellini, and L. Reining, Solid State Commun. **84**, 765 (1992).
[33]P. Lautenschlager, M. Garriga, and M. Cardona, Phys. Rev. B **36**, 4813 (1987).
[34]K. Hingerl, D. F. Aspnes, I. Kamiya, and L. T. Florez, Appl. Phys. Lett. **63**, 885 (1993).
[35]P. Lautenschlager, M. Garriga, and M. Cardona, Phys. Rev. B **36**, 4813 (1987).
[36]P. Lautenschlager, M. Garriga, S. Logothetidis, and M. Cardona, Phys. Rev. B **35**, 9174 (1987).